https://doi.org/10.20965/ijat.2019.p0207

Technical Paper:

Mirror-Surface Finishing by Integrating Magnetic-Polishing Technology with a Compact Machine Tool

Yuki Manabe*,†, Hiroki Murakami*, Toshiki Hirogaki*, Eiichi Aoyama*, and Tatsuya Furuki**

*Graduate School of Science and Engineering, Doshisha University
1-3 Tataramiyakodani, Kyotanabe-shi, Kyoto 610-0394, Japan
†Corresponding author, E-mail: y.manabe.dss@gmail.com
**Graduate School of Engineering, Gifu University, Gifu, Japan
[Received June 30, 2018; accepted February 8, 2019]

In recent years, owing to the advent of mobile phones, product miniaturization and multifunctionalization have rapidly progressed. However, the large-sized machine tools for the manufacture of small products waste a considerable amount of space and power. The present study aimed at applying a magnetic-polishing method using a ball-end mill-type tool to examine the optimum processing conditions. This was done to apply a mirror finish for the integration of the cutting and polishing processes by using the small machine tool. The magnetic-polishing effect was evaluated from the point of view of the polishing amount, surface roughness, specimen shape, and mirror-surface condition. In addition, the movement of the paste during polishing was observed through images obtained through a high-speed camera. The movement of the paste is considered for effective polishing and other cases. Accordingly, various magnetic-polishing techniques were used for irregularities and step shapes. Various conditions were also examined, and a stable condition was determined. The results reveal that the amount of polishing paste significantly influences the polishing movement. In addition, a sufficient polishing effect could be obtained by duplicating the polishing course by using a sine wave course.

Keywords: magnetic polishing, mirror finish, compact machine tools

1. Introduction

Consumer goods of daily use are becoming increasingly smaller and lighter [1], and processing requirements that can be adapted to small parts composing these productive goods are increasing. However, the sizes of machines (e.g., machine tools and industrial robots) have not changed significantly, and even for small products, large machines are often used. These large machine tools occupy large spaces and consume high amount of power, thereby leading to wastage problems [2]. In response, the miniaturization of machine tools has been recognized as an effective means of reducing the absolute global-warming index in the manufacturing processes and in the use of machine tools. The processing of a small part generally requires the use of a processing method suitable for the size of the part [3]. Solutions to this problem have led to production downsizing and implementation of cell production systems [4, 5]. This idea is also useful from the point of view of life-cycle assessment (LCA) [6, 7]. LCA is a method to calculate not only the power consumption during product processing but also the cost of manufacturing and disposing of processing machines. Smaller processing machines are considered advantageous because such machines help reduce the use of materials and power consumption for each production considering manufacturing processes.

The integration of cutting and polishing processes in small machine tools has been proposed for the use of cell production and LCA concepts. This research proposed a magnetic-polishing method by using a small-diameter ball-end mill-type polishing tool [8, 9]. The aim of the research was to integrate cutting and polishing processes by using one compact machine tool [10, 11]. These studies reported on R5, which can be easily used to keep the magnetic force large. However, the use of a small tool is advantageous for performing detailed polishing. Therefore, in this study, experiments were conducted by using R2 tools. In addition, the effect of the magnetic-polishing method on the groove shape was considered from the point of view of the polishing amount (removal mass) before and after polishing, surface roughness, polished surface shape, and mirroring. An examination of the processing conditions for achieving the mirror finish through the proposed magnetic polishing was performed based on the results. Although the magnetic-polishing method has been shown to be effective in previous studies [12, 13] with respect to the groove shape, when the height and width of the groove shape decrease or achieve a certain size, a sufficient polishing effect cannot be obtained inside the groove in the dynamic equilibrium steady state of the polishing magnetic paste. Therefore, to cope with the direct product manufacture (groove shape) as well

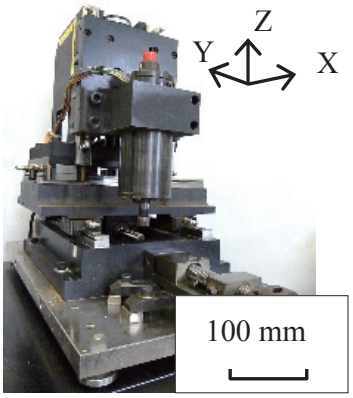

Fig. 1. Desktop-sized CNC machine tool, MM 55.

as manufacturing the product from a metal mold (step shape), a groove-step shape was developed in this study by adding the step shape to the groove shape. An improvement was confirmed by oscillating (swinging) the magnetic-polishing paste in an unsteady state by using the new polishing method.

2. Experimental Methods

2.1. Experimental Equipment

A three-axes orthogonal-type vertical compact CNC machine tool (MM 55) from Iwama Kogyo Co., Ltd. (**Fig. 1**) was used for the groove and step cutting and magnetic polishing. The installation floor area was 0.183 m^2, and the weight was approximately 40 kg. Considering that the machine weight in a conventional machine tool often exceeds 5 t, this machine tool was extremely small and lightweight. Its operating range was 50 mm × 50 mm × 50 mm. After processing, the test piece was washed with ethanol by using an ultrasonic washer manufactured by Velvo-clear (40 kHz) to remove all foreign matter from the surface of the workpiece. Thereafter, the roughness (*Ra*, *Rz*) and shape of the polished surface were measured before and after magnetic polishing by using a laser-type shape-measuring instrument, VK-X 210 (Keyence) and a stylus shape-measuring instrument HandySurf E-35B (Tokyo Seimitsu Co., Ltd.).

2.2. Tools, Magnetic-Polishing Paste, and Workpiece

A double-bladed square-end mill MS 2 SS (Mitsubishi Materials Corporation) with blade diameters of $De = 1.0$ and 6.0 mm were used for the groove and step shape cutting, respectively. For the polishing process, abrasive grains (i.e., alumina and stainless steel; **Fig. 2(b)**) were applied to a ball-shaped magnetic-polishing tool (NPS-φ3-φ4-R2 from FDK) with a ball-tip radius of $R_p = 2$ mm (**Fig. 2**) and a magnetic-polishing paste (MPL-CU 3 LBOD from FDK) comprising magnetic metal particles (iron; average particle diameter $\varphi =$ 50 μm) and a solvent (vegetable oil/fat) were used to form the magnetic-polishing brush [14]. The conditions of the paste are summarized in **Table 1**, which shows that the alumina particles are only approximately 1/1000-th of the size of the iron particles. Therefore, the alumina particles were adsorbed by iron particles through the surface tension of the oil, carried toward the outer circumference by the centrifugal force generated in iron particles, and collided with the workpiece [9].

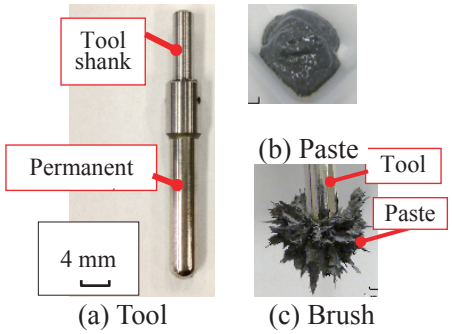

Fig. 2. Magnetic-polishing tool.

Table 1. Paste information.

	Almina	Iron	Oil
Mass [wt%]	37.5	37.5	25
Diameter [μm]	0.05	50	–
Density [kg/m^3]	7860	3950	950

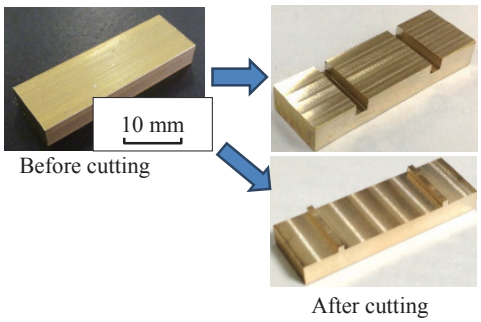

Fig. 3. Workpiece (brass).

The tip of the polishing tool was a strong neodymium permanent magnet; hence, the workpiece was made of a nonmagnetic metal (brass workpiece of 30 mm × 10 mm × 5 mm, as in **Fig. 3(a)**) so that it could not be affected by the magnetic force. Because cutting was to be performed, stainless-steel-like materials, which are difficult to cut, were avoided. **Fig. 3(b)** shows the groove- and step-shaped workpieces after machining. Two channel shapes were prepared on one workpiece so that the other face was not affected during polishing. The width of both the groove and step shapes was $b = 1.0$ mm. The height $h = 1.0$ mm and length $y = 10$ mm were according to the

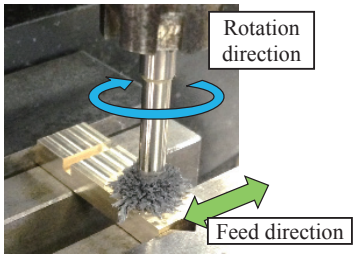

Fig. 4. Channel polishing.

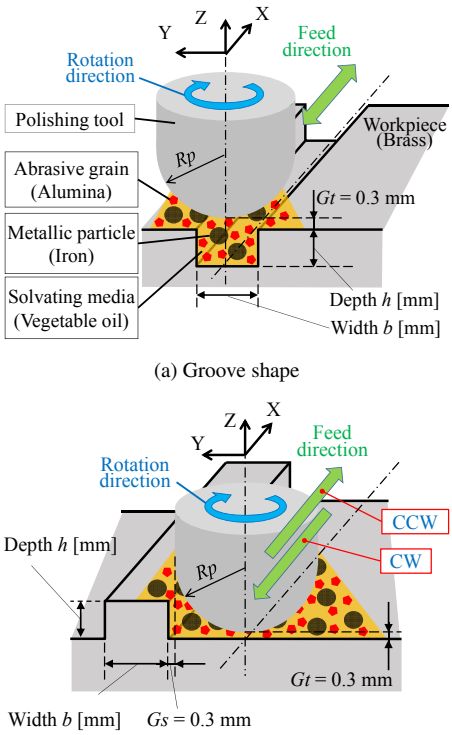

(a) Groove shape

(b) Step shape

Fig. 5. Polishing method.

tool diameter used for groove cutting. **Fig. 4** illustrates the experimental state when using the groove shape. In the experiment, magnetic polishing of the workpiece was done under the same conditions for two identical shapes. The mass, surface roughness (central average roughness Ra, maximum roughness Rz), and shape of the polished surface were measured before and after polishing. The surface roughness is an average value measured at three places in each of two shapes.

2.3. Experimental Conditions

To create grooves, a two-blade square-end mill with a diameter of 1 mm was used. Its rotation speed was 16,000 rpm and feed speed was 400 mm/min. Additionally, to create steps and planes, a 6-mm-diameter double-bladed square-end mill was used with a rotation speed of 12,800 rpm and feed speed of 400 mm/min (tool manufacturer recommended value).

Figure 5 shows the system of the magnetic-polishing

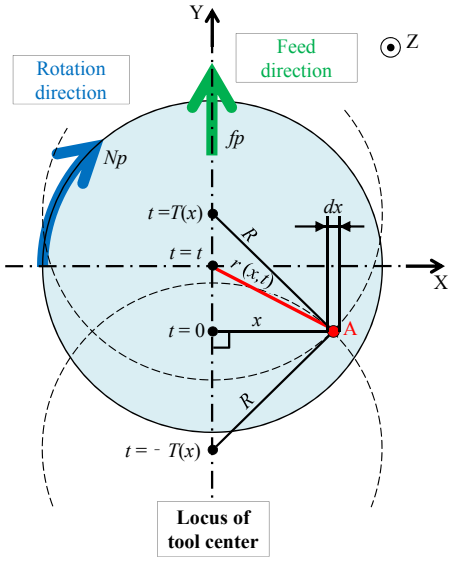

(a) Movement

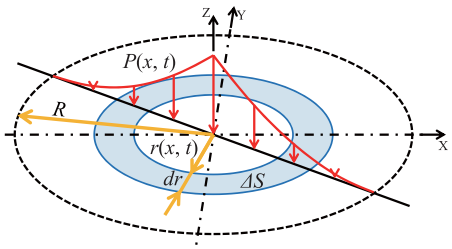

(b) Pressure

Fig. 6. Magnetic-polishing brush model.

method used in this study. The feed rate was $f_y = 10$ mm/min, as represented by the Y-axis. The gap (i.e., the distance between the polishing tool tip and the workpiece top face) was $G_t = 0.3$ mm. For the step shape, $G_s = 0.3$ mm from the side face and 0.3 g of the paste was used. The polishing tool and workpiece were always in a noncontact state. The paste followed the rotation and feed motion of the polishing tool and deformed according to the workpiece shape. Moreover, both the bottom and the side surface were polished because the abrasive grains in the paste moved along the polishing surface.

3. Polishing Theory for Magnetic Brush

The Preston formula presented in Eq. (1) was used to predict the amount of polishing in the magnetic-polishing process [15, 16].

$$M' = kPv_t. \quad \ldots\ldots\ldots\ldots\ldots\ldots \quad (1)$$

In **Fig. 6(a)**, R is the radius [mm] of the contact between the polishing brush and the surface to be polished, and x is the perpendicular distance [mm] between point A and the center trajectory of the polishing tool, $r(x,t)$ [mm]. The distance between point A and the center of the polishing tool was measured after 2 s. The polishing time for point A is represented by $2T(x)$ [s], assuming that $t = 0$

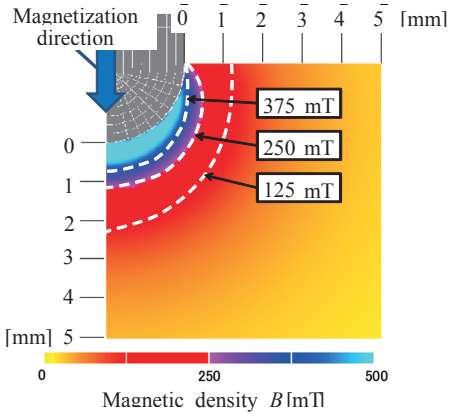

Fig. 7. Magnetic field distribution.

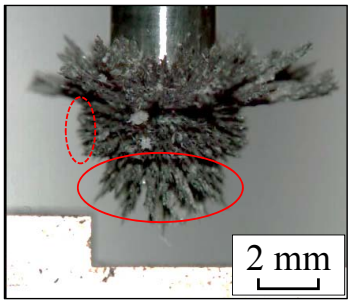

Fig. 8. Paste shape after polishing.

when $r = x$. The following equation is obtained when this motion model is applied to Eq. (1):

$$M = 4ky \int_0^R \int_0^T Pv \, dtdx, \quad \ldots\ldots\ldots \quad (2)$$

where M [mg] is the removal mass (polishing amount) and y [mm] is the polishing distance.

Next, to obtain the polishing pressure, the magnetic force distribution was calculated from the data provided by the tool maker. The result is presented in **Fig. 7**, which shows that the paste is generally gripped in an elliptical shape. Further, the shape of the paste was observed while polishing the step, as shown in **Fig. 8**, where the tool is raised vertically after rotation. The distance of the tool from the step is 0.3 mm and the rotation time is 60 s. The solid part of the paste shape, as shown in **Fig. 8**, is assumed to be rotating without considering its flowability. Furthermore, the figure shows that a large amount of paste is distributed in the part surrounded by the solid line, and a polishing pressure is generated. However, the side surrounded by the broken line shows that the paste is distributed in the same shape as in the step, and almost no polishing pressure is generated. Thus, we decided to consider only the polishing of the bottom surface.

In this study, polishing pressure P [MPa] was assumed to be represented by a quadratic function of radius r [mm], as shown in **Fig. 6(b)**:

$$P = C(r-R)^2, \quad \ldots\ldots\ldots\ldots\ldots \quad (3)$$

where C is a constant. The polishing load (i.e., the load applied in the negative direction of the Z-axis in **Fig. 5**) F_z [N] applied within the paste contact range is expressed as follows:

$$F_z = \int P \cdot \Delta S$$

$$= \int_0^R C(r-R)^2 \cdot \pi \left\{ (r+dr)^2 - r^2 \right\} = \frac{\pi}{6} CR^4, \quad (4)$$

where ΔS [mm^2] is a minute contact area between the polishing brush and the surface to be polished. Therefore, from Eqs. (3) and (4), polishing pressure P becomes

$$P = \frac{6F_z}{\pi R^4}(r-R)^2. \quad \ldots\ldots\ldots\ldots \quad (5)$$

In this study, pressure P was calculated by measuring F_z through a force sensor. In **Fig. 6(a)**, distance $r(x,t)$ between point A after t seconds and the center of the polishing tool and half $T(x)$ [s] of the polishing time for point A become

$$\begin{cases} \sqrt{r(x,t)^2 - x^2} = \dfrac{f_p}{60} t \\ r(x,t) = \sqrt{x^2 + \left(\dfrac{f_p}{60} t \right)^2}, \end{cases} \quad \ldots\ldots\ldots \quad (6)$$

$$T(x) = \frac{60\sqrt{R^2 - x^2}}{f_p}, \quad \ldots\ldots\ldots\ldots \quad (7)$$

where f_p [mm/min] is the feeding speed of the polishing tool in the direction of the Y-axis.

The polishing relative speed, represented by $v(x,t)$ [mm/s], is expressed as in Eq. (8) because the speed of the movement of the polishing tool in the experimental conditions was so small that the feed speed was negligible with respect to the peripheral speed:

$$v(x,t) = \frac{2\pi N_p}{60} \cdot r(x,t), \quad \ldots\ldots\ldots\ldots \quad (8)$$

where N_p [per min] is the rotation speed of the polishing tool.

4. Experimental Results and Discussion

4.1. Magnetic Polishing for Planar, Groove, and Step Shapes

4.1.1. Experiment Outline

In a previous study [17], the polishing effect was verified by performing magnetic polishing on planar and groove shapes. However, the roughness of the bottom of the groove was not improved. Furthermore, the product may have both the groove and step shapes. Therefore, in this study, magnetic polishing was performed on a step-shaped workpiece to observe the application of the proposed method over a wider range of shapes. An appropriate polishing condition was also examined from the verification result of the polishing effect.

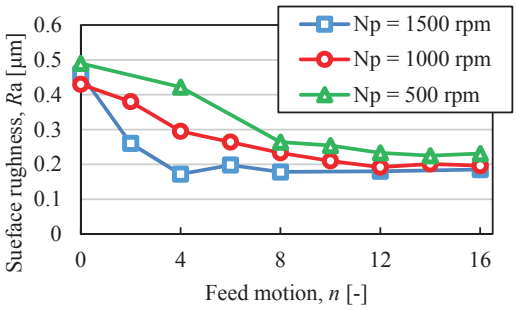

Fig. 9. Influence of feed motion n under various rotation speeds N_p on surface roughness.

First, magnetic polishing in a steady state was performed on flat, groove, and step shapes, as in [17]. The difference in the polishing effect was then compared depending on the presence or absence of concavities and steps. **Fig. 4(b)** shows the shape of the workpiece, with a channel width of $b = 1.0$ mm and heights of $h = 0.3$ and 1.0 mm. **Fig. 5(a)** shows that the groove shape was polished in a linear reciprocating motion such that the center of the polishing tool was aligned with the groove center. **Fig. 5(b)** demonstrates that the step shape was polished by a linear motion in one fixed direction through a one-step difference. In the scanning direction, polishing was performed around the step shape in two directions: the same direction (counterclockwise, CCW) as the tool-feeding direction, and the rotating direction of the polishing paste in the opposite direction (clockwise, CW). The feed speed in all conditions was constant at $f_y = 10$ mm/min in the direction of the Y-axis. The distance from the tip of the tool to the bottom of the groove step was 0.6 mm. Moreover, the plane gap was determined to be 0.6 mm for comparison.

An experiment was conducted to find the number of polishing passes, n, required for a sufficient polishing effect for a polishing rotational speed of N_p during the experiment against a flat surface without irregularities. **Fig. 9** shows the measurement results of surface roughness Ra [μm] for the rotational speeds of $N_p = 500$, 1000, and 1500 min^{-1}. **Fig. 9** shows that the result with the rotation speed of 1500 rpm was the best; however, the authors found that almost the same polishing roughness can be obtained by increasing the number of polishing rounds. In the magnetic-polishing method, if the rotation speed is too large, the paste may get scattered because of the centrifugal force at the start of the tool rotation. Although the paste scattered at 1500 rpm and not at 1000, 500 rpm (at which the paste does not scatter at all) was judged suitable for observation. Furthermore, in [11], the theoretical polishing amount (bottom surface) of the groove-shaped polishing decreased (which was considered better) with a decrease in the rotation speed. The polishing effect (surface roughness) was obtained as a result of actually polishing at the rotation speed of $N_p = 500$ min^{-1}. Therefore, the optimum rotation speed during polishing was taken as $N_p = 500$ min^{-1}. However, the experiment was conducted with $N_p = 500$ and 1500 min^{-1} because the manufacturer recommended rotation speed of the tool was approximately $N_p = 1500$ min^{-1}. The number of polishing rounds at which the change became small at 500 rpm was determined to be 12.

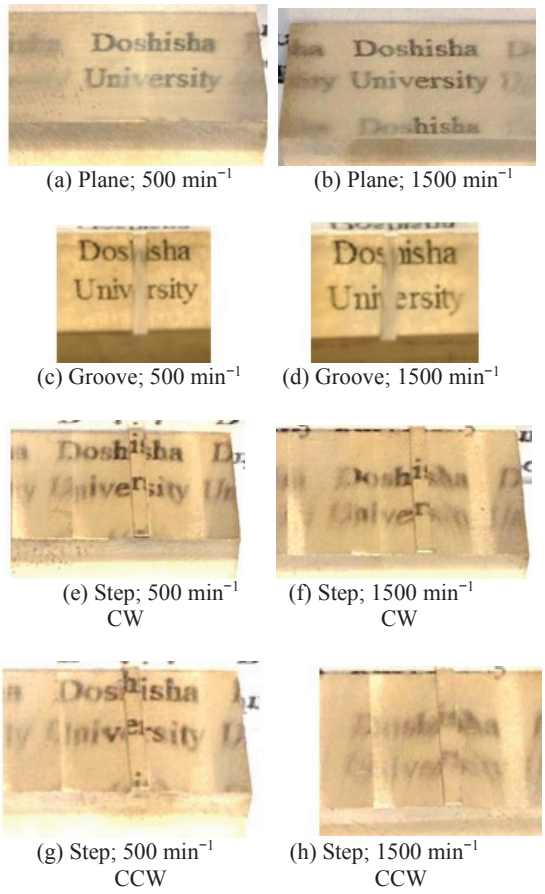

Fig. 10. Surfaces after magnetic polishing.

4.1.2. Experimental Results

Figure 10 shows the result of polishing for a groove depth of 0.3 mm; the same tendency was observed for the groove depth of 1.0 mm. **Figs. 10(a)** and **(b)** show images of the surface after planar polishing; **Figs. 10(c)** and **(d)** show the surface after groove polishing; and **Figs. 10(e)–(h)** show the surface after step polishing. **Figs. 10(c)** and **(d)** confirm that although the groove depth is just 0.3 mm, the bottom surface cannot be polished. **Fig. 11** presents the respective polishing amounts. By judging the polishing result through visual observation, the sharpness of the reflected character string can be confirmed [18, 19]. In this study, the character string "Doshisha University" was reflected. Regarding the mirror-surface degree, the roughness before polishing (i.e., the character string was blurred) was approximately $Ra = 0.46$ μm and $Rz = 2.25$ μm, as obtained from the magnetic-polishing result with respect to the plane, and $Ra = 0.18$ μm and $Rz = 0.83$ μm after polishing (i.e., the character string was sufficiently clear). Therefore, the

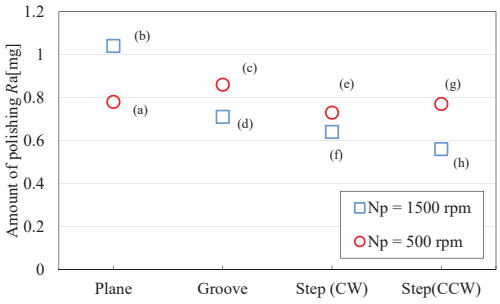

Fig. 11. Influence of the surface shape on the amount of polishing.

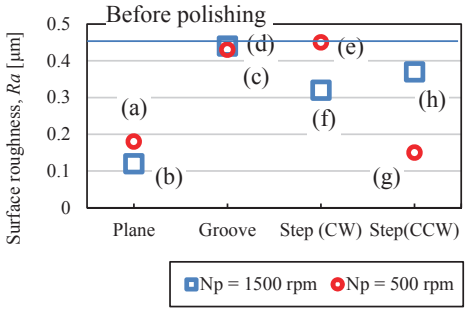

Fig. 12. Surface roughness after magnetic polishing.

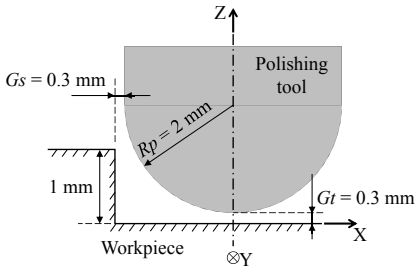

Fig. 13. Tool position.

mirror-surface degree after polishing was considered to be *Ra* and *Rz* values when the character string is clear.

In the case of planar polishing, as shown in **Figs. 10(a)** and **(b)**, $N_p = 1500$ min^{-1} with a larger rotation speed showed a slightly clearer character string and a larger polishing amount. Compared to the rotational speed employed in ordinary grinding-wheel polishing, a higher rotational speed was more effective in planar polishing. However, the scattering of the paste was observed during higher rotation speeds.

Further, in the case of groove-shaped polishing, as shown in **Figs. 10(c)** and **(d)**, the top surface of the workpiece was polished, but the bottom surface of the groove was insufficiently polished as in the previous study. In **Fig. 11**, although the amount of polishing was obtained to be of the same extent as that for the flat surface, most of the polishing was done for the top surface of the workpiece (other than the groove) with respect to the mirror surface degree. In the case of step-shaped polishing, **Figs. 10(e)–(h)** depict that the character string was clearer when $N_p = 500$ min^{-1}, and the polishing amount was approximately the same as that for the flat surface.

For the uneven shape, the polishing paste needed to enter the groove or a corner. Therefore, the centrifugal force caused by the rotation increased more than the pressing force exerted by the magnetic force. When grinding the groove shape, it takes time for the paste on the top surface of the groove to move to the bottom of the groove. Therefore, at high speed rotation, it is considered that the paste moves to the top surface of the next groove before the paste moves to the bottom surface of the groove. The step shape achieved its step shape again before the paste fell to the bottom surface; hence, it was difficult for the paste to reach the lower part of the corner. As a result, the polishing effect was very less. Therefore, to obtain the polishing effect for uneven shapes equivalent to that of a flat shape, N_p must be 500 min^{-1} at a low rotation speed. Furthermore, for the step-shaped polishing (CW, CCW), the CCW rotation, in which the relative polishing speed was increased, was adopted because no significant difference was found when $N_p = 500$ min^{-1}, which provided the polishing effect. **Fig. 12** shows the surface roughness at this time. The visual observation results show that the surface roughness values of groove and step polishing are poorer than that of planar polishing. In addition, considering that the surface roughness before polishing was approximately $Ra = 0.4$ μm, almost no polishing can be observed.

4.2. Motion State of Polishing Paste During Polishing on Steps

4.2.1. Experimental Overview of the Observation from the Side Surface of Step

The shape of the magnetic fluid polishing paste varied according to the workpiece shape. Iron particles formed into clusters through the magnetic flux of the polishing tool and attached to abrasive grains. In planar polishing, the clusters could maintain almost the same state. However, in the uneven-shape polishing, the clusters collapsed on coming in contact with the channel, thereby resulting in an irregular movement. Therefore, the polishing effect of the magnetic polishing on the uneven shape and the motion state of the polishing paste differed considerably from those observed in planar polishing.

Therefore, the paste movement during the rotation of the polishing tool was observed to elucidate the motion on the uneven shape. The groove-step shape can be regarded as a combination of two step shapes divided at the center; therefore, the ease of observation from the lateral direction was considered, and the brass-based step shape was observed after this experiment. The step was 2.0-mm high (**Fig. 13**), and polishing was performed by separating the polishing tool from each surface by 0.3 mm from the side surface and the step bottom surface. This experiment did not consider the feed motion ($f_y = 0$). Moreover, the paste motion for tool rotation was considered only from the side and bottom directions through a high-speed camera (i.e.,

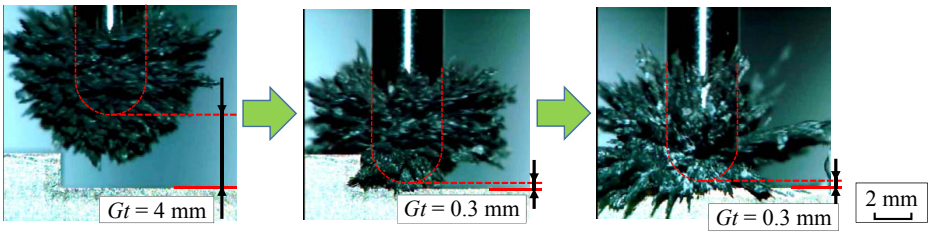

(a) 0.5-g paste

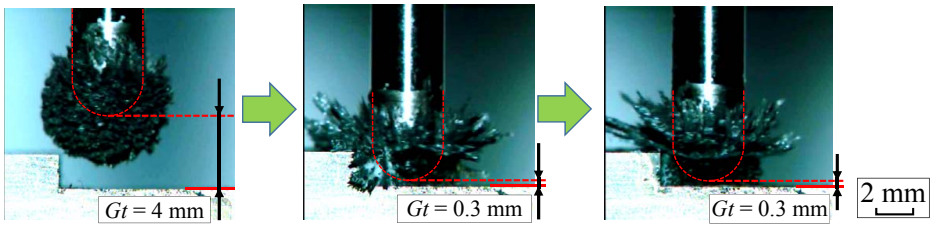

(b) 0.3-g paste

Fig. 14. Side-view of paste motion.

VW-9000, Keyence) with a shutter speed of 1/3000 s and frame rate of 500 fps.

4.2.2. Experimental Results

Figures 14(a) and **(b)** show images of the motion states of the 0.5-g and 0.3-g pastes (before contacting → 5 s after reaching the *Z*-axis command value → 10 s after reaching). Much of the 0.5-g paste accumulated at the corners and did not follow the tool rotation. The following paste also ran on the accumulated paste without hitting the side face. This process continued during polishing; hence, the amount of polishing on the side and bottom surfaces of the portion where the paste accumulated decreased. The overall polishing effect also decreased. Therefore, not only the shape of the workpiece, but also the polishing paste caused the polishing motion to be obstructed.

Figure 14(b) depicts the observation result of 0.3-g paste, which was thought to be less excessive than the 0.5-g paste. A paste pool was observed immediately after initiating rotation, but it decreased after a few seconds, and the paste followed along the workpiece shape. The paste was applied to the polished surface as the rotation stabilized. **Fig. 8** shows the paste (0.3-g paste) separated from the workpiece after polishing for 60 s.

The abovementioned results and those from **Fig. 15** indicate three distinct regions: (I) the top surface of the workpiece, (II) the strong-magnetic-flux region inside the groove (just under the polishing bit), and (III) the weak magnetic-flux-density regions separated from each other.

The 0.5-g paste in region (I) rotated only above the top surface of the workpiece and did not participate in polishing of the inside of the groove. No change was observed in the paste shape; therefore, the part in contact with the top surface polished the top surface. The paste in region (II) polished the side and bottom surfaces inside the groove. In region (III), the paste that could not follow the tool rotation accumulated in the corner, and the following paste

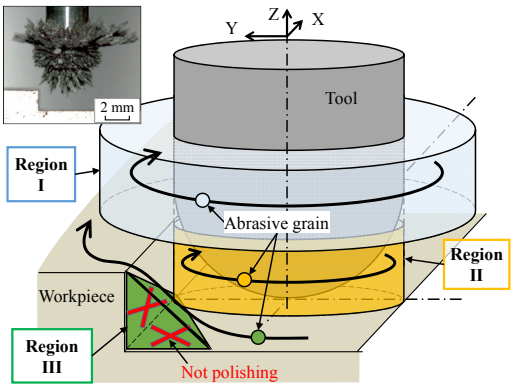

Fig. 15. Paste model during polishing.

ran over it and rotated because the effect of the magnetic flux density of the polishing tool was very small. Consequently, the paste did not come into contact with the side surface, except initially, and almost no polishing effect was obtained.

Regions (I) and (II) showed similar results for the 0.3-g paste; however, no change was observed in region (III) because unlike for the 0.5-g paste, additional paste did not exist for the 0.3-g paste. As a result, the rotational motion of the paste within region (II) was stabilized and was in contact with a wide range of the side surface, thereby improving the polishing effect.

4.3. Motion State Near the Tool Center of the Polishing Paste During Polishing

4.3.1. Outline of the Experiment for Observation from the Bottom of the Groove Using an Acrylic Plate

In Section 4.2, the paste movement was observed only from the lateral direction. The motion state of the paste in the vicinity of the tool cannot be observed from the axial direction because brass was used for the work.

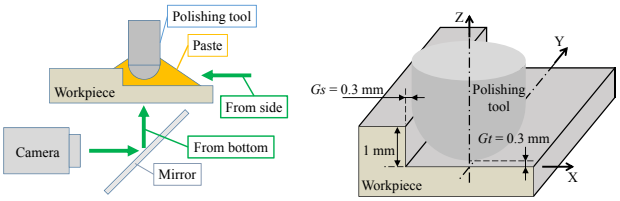

Fig. 16. Monitoring method of the paste motion through clear acrylic resin (step shape).

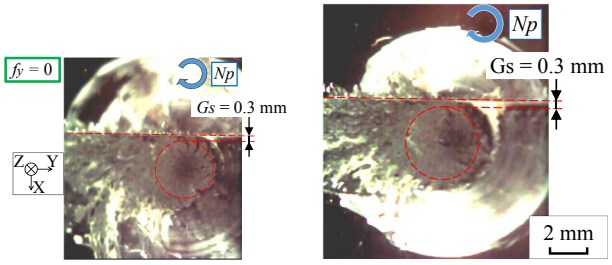

(a) 0.5-g paste (b) 0.3-g paste

Fig. 17. Bottom view of paste motion.

Accordingly, a step shape was constructed using a transparent acrylic plate to enable observation from the axial direction. Section 4.2 discussed how a high-speed camera was used to capture motion pictures for 0.3-g and 0.5-g pastes. **Fig. 16** shows the positional relationship among the polishing tool, workpiece, and camera when taking photographs from the bottom side.

4.3.2. Experimental Results

Figure 17 shows a photograph taken with the high-speed camera from the bottom surface of the paste motion with only tool rotation and no feeding motion ($f_y = 0$). In the case of the 0.5-g paste, **Fig. 17(a)** shows that the paste accumulated at the corner, as discussed in Section 4.2, whereas the 0.3-g paste rotated. However, when observing the rotational motion of the paste near the center from the lower side of the workpiece, the rotational speed of the paste was much slower than that of the spindle. Furthermore, the rotating and stationary states were intermittently repeated, showing many moments that were particularly stationary. The paste was pulled by a magnetic force in the circumferential direction to follow the bite rotation. However, the amount of paste accumulated in the corners was large when a large paste amount was used. The magnetic force also acted between the accumulated paste and the polishing tool to form paste clusters such that the effect of the magnetic force was applied to the paste rotating between the two exits. The directions of these two magnetic forces were almost vertical; therefore, the force caused by the rotation was weakened. This was considered to be the cause of the instability caused by the delay in the rotation around the tool center. Therefore, most of the paste was used up in polishing.

In contrast, in the case of the 0.3-g paste, as shown in **Fig. 17(b)**, although some paste accumulation did occur,

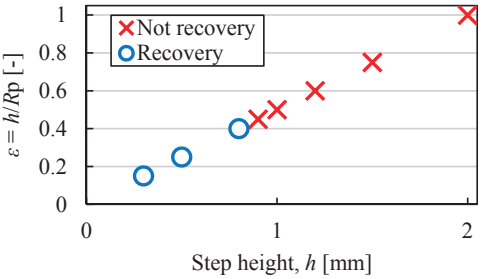

Fig. 18. Relationship between h and R_p.

no magnetic force was observed between the accumulated paste and the tool, unlike in the case of the 0.5-g paste. Therefore, the vicinity of the tool center rotated stably.

Therefore, with respect to the stepped shape, obtaining the magnetic-polishing effect under the same conditions as those of the flat polishing was difficult. In addition, obtaining a polishing effect by changing the paste amount according to the shape of the polished surface (e.g., height) was difficult. This was effective for improving the effect. Under this condition, the polishing effect can be improved by decreasing the paste amount, and a sufficient effect can be expected when using the 0.3-g paste. In addition, by examining the conditions under which step height h [mm] was varied to produce paste accumulation, the relationship between step height h and polishing tool diameter R_p [mm] is represented by $\varepsilon = h/R_p$. Paste accumulation occurred continuously when $\varepsilon \geq 0.45$ or more. Therefore, the subsequent polishing conditions can be applied to the condition of $\varepsilon \approx 0.45$ or more. **Fig. 18** shows the results of investigating the state of paste pool at various step heights. The ratio of the radius of the polishing tool to the height of the step height was taken as the ordinate, making it dimensionless. As can be seen from **Fig. 18**, it has been found that the paste pool cannot be eliminated when the height of the step height exceeds a certain level.

4.4. Investigation of Polishing Conditions for Step Shape

4.4.1. Experimental Overview of the Addition of Vertical Motion Perpendicular to the Feed Direction of the Tool

The rotational motion of the paste around the polishing tool can be stabilized by adjusting the paste amount according to the shape, as discussed in Section 4.3. However, when polishing the stepped shape, both the bottom and side surfaces must be polished. Here, the paste is accumulated only through the linear motion; hence, the contact range of the paste with the side surface can decrease, and a sufficient polishing effect may not be obtained.

For efficiency, instead of going back and forth many times by the linear feed, we consider a path that can obtain sufficient polishing effect in one reciprocation and eliminate paste accumulation [20]. Two paths were examined in the horizontal direction with respect to the feed

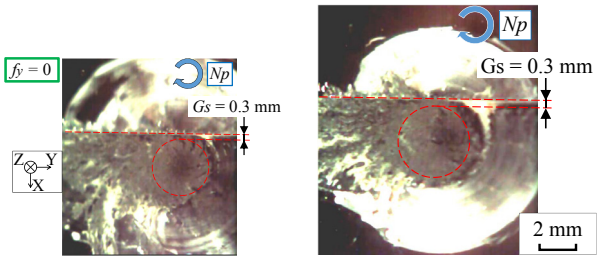

Fig. 19. Pass routes (step): (a) horizontal direction (X-Y surface) and (b) vertical direction (Y-Z surface).

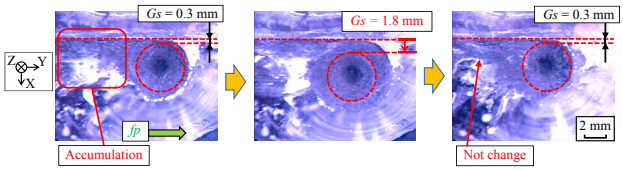

Fig. 20. Bottom view of the movement in the horizontal direction (from left: when straight fed; 1.5 mm away in the Y-direction; returning to the original distance).

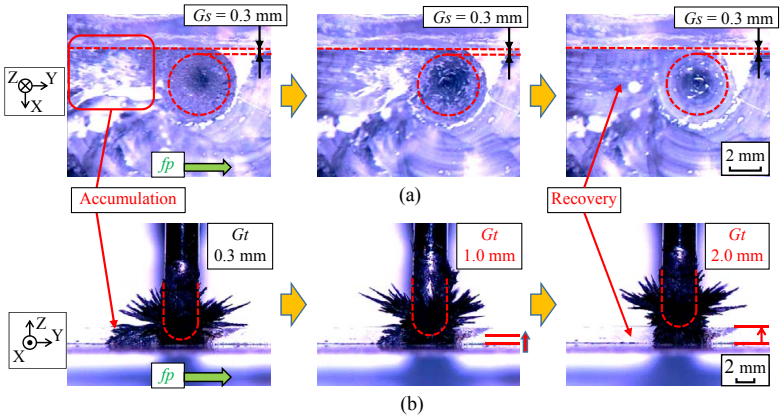

Fig. 21. (a) Bottom and (b) side views of movement in the vertical direction (from left: when linearly fed; G_t = 1.0 mm, increased by 0.7 mm in the Z-direction; G_t = 1.7 mm, increased by 2.0 mm in the Z-direction).

direction of the tool (displacement on the X-Y plane in **Fig. 19(a)**) and in the vertical direction (displacement on the Y-Z plane in **Fig. 19(b)**). The workpiece was an acrylic plate of height $h = 2.0$ mm and was photographed from the side and bottom by using the high-speed camera under the same conditions as those shown in **Fig. 16**. After observing the paste motion on the acrylic plate, the actual polishing effect was confirmed on brass. The feed speed in this experiment was set to be the same in the feed direction (Y-axis) and additional directions (X- and Z-axes) as $f_x = f_y = f_z = 10$ mm/min.

4.4.2. Experimental Results of the Effect of the Z-Axis Vertical Motion

Figure 20 shows bottom view photographs with respect to displacement in the horizontal direction. Images from the side were omitted because they did not exhibit any change. In addition, as shown in **Figs. 21(a)** and **(b)**, photographs were taken from the bottom and side surfaces, respectively, when displaced in the vertical direction. As shown in **Fig. 20**, in the case of the horizontal direction, even for a displacement in the Y-direction, the paste accumulation did not move, and there was no improvement; i.e., its state of contact with the side surface did not change. The volume of the gap resulting from the amount of displacement (approximately 12 mm × 3 mm in this condition) was smaller than the volume of the paste reservoir (approximately 16 mm × 3 mm according to the photograph); therefore, this problem was not solved completely. Some of the real products for groove-shaped polishing have microchannels arranged in parallel; therefore, increasing the amount of displacement in the horizontal direction and the application of the horizontal path to eliminate the paste pool were difficult. In contrast, almost no restrictions were observed on the range of ascent in the case of the vertical direction irrespective of the shape of irregularities. Therefore, by raising the polishing tool in the Z-direction by G_t = 1, 2, 3, and 5 mm, as shown in **Fig. 21(b)**, the accumulation of the paste was eliminated. All paste accumulation can be recovered with a gap of $G_t \geq 2.0$ mm at the same level as the step. At $G_t = 2.0$ mm, a clearance of approximately 25 mm × 3 mm was generated under the polishing tool; hence, a stable rotational motion, including additional paste, was possible.

The paste puddle was temporarily eliminated by raising the polishing tool; however, it returned to the original state when the tool was lowered again to the original height $G_t = 0.3$ mm. However, the polishing effect can be expected to improve because the paste again came into contact with the side and bottom surfaces. The polishing time can be decreased because of the smaller amount of

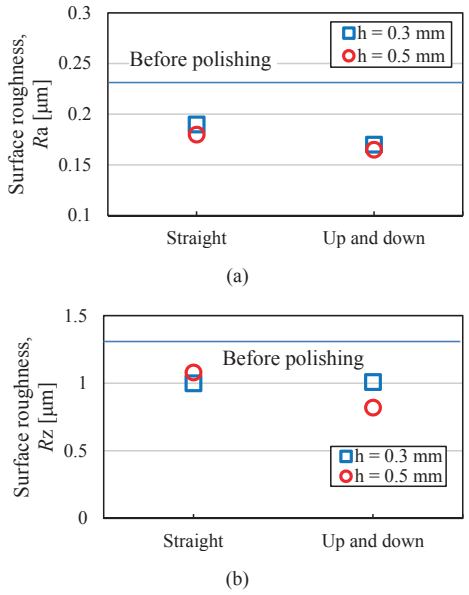

Fig. 22. Surface roughness for (a) *Ra* and (b) *Rz*.

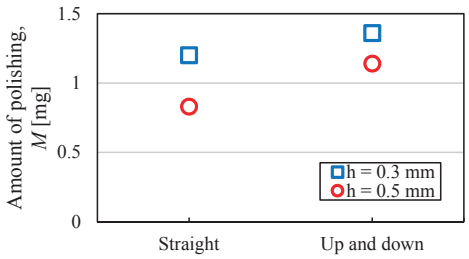

Fig. 23. Amount of polishing.

displacement in the Z-direction. Hence, raising the tip of the polishing tool to the same height as that of the step was sometimes necessary in the Z-direction (e.g., step cycle feed of drilling to eliminate the pool). This move was considered to be effective.

Next, a brass specimen cut into a step shape was polished using the method shown in **Fig. 19(b)** to confirm the actual polishing effect on brass. The step height was set to $h = 0.3$ and 1.0 mm, and vertical movement feed was made at 3.0-mm intervals in the Y-direction. **Fig. 22** shows the surface roughness *Ra* and *Rz* before and after polishing, respectively. **Fig. 23** shows polishing amount M [mg]. **Figs. 22** and **23** show that, in the experiment on the acrylic plate (Section 4.3), the addition of an "up-down motion feed" rather than a "simple straight feed" raised the tool tip by 1° in the Z-direction from time to time to recover the paste, resulting in improvement in the surface roughness and increase in the polishing amount. **Fig. 23** shows that the change in the polishing amount of $h = 0.3$ mm was small because the step height was smaller than the diameter of the polishing tool. Consequently, the shape of the polishing paste was not substantially influenced by the workpiece shape.

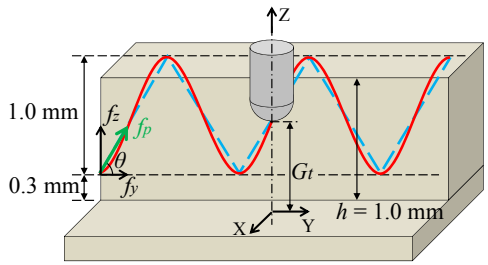

Fig. 24. Experimental condition.

4.5. Polishing and Theoretical Expression with Oscillation Motion

4.5.1. Experiment Outline for Adding Vertical Oscillation Motion Perpendicular to Feed Motion

Section 4.4 discussed that any motion other than a straight-line motion was effective for polishing with the addition of a vertical motion perpendicular to the tool feed direction. However, in the vertical motion, polishing took time, and its efficiency worsened because it did not advance in the feeding direction until after returning to the original tool tip height. Therefore, we examined polishing in the vertical path by using the sine wave to simultaneously perform the upper and lower oscillations and the feeding motion. However, for the ease of programming, experiments were conducted using a triangle wave approximation. In experiments using actual machine tools, the triangle wave approximation was implemented through a linear interpolation motion at a constant angle of course [deg]. As shown by the dotted line in **Fig. 24** and considering the ease of setting at the site, the return path was shifted by half a cycle. At this time, the triangular wave is represented by the following equation:

$$\begin{cases} \left(-\dfrac{h'}{\tan\theta} < x \leq -\dfrac{h'}{2\tan\theta}\right) \\ \qquad f(x) = -\tan\theta \times \left(x + \dfrac{h'}{2}\right) + G, \\ \left(-\dfrac{h'}{2\tan\theta} < x \leq \dfrac{h'}{2\tan\theta}\right) \\ \qquad f(x) = -\tan\theta \times x + G, \\ \left(\dfrac{h'}{2\tan\theta} < x \leq \dfrac{h'}{\tan\theta}\right) \\ \qquad f(x) = -\tan\theta \times \left(x - \dfrac{h'}{2}\right) + G. \end{cases} \quad . \quad (9)$$

Here, h' is the height of the vertical movement of the magnetic tool and G is the distance from the bottom surface when the magnetic tool is at its lowest position. The workpiece was shaped as a step with height $h = 1.0$ mm. The displacement width of the polishing tool was 1.0 mm, and angle θ of the triangle wave approximation was based on a polishing time of 0.8 min/mm per unit polishing dis-

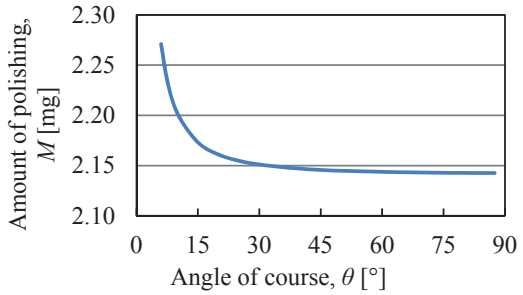

Fig. 25. Amount of polishing before considering overlap.

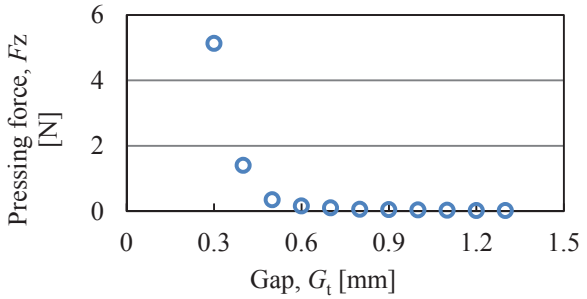

Fig. 26. Relationship between G_t and F_z.

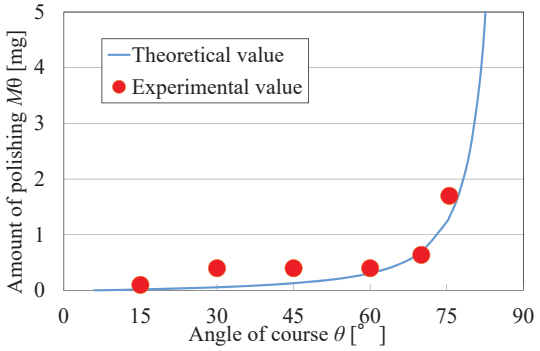

Fig. 27. Amount of polishing after considering overlap.

tance, which obtained a sufficient polishing effect through plane polishing (i.e., 75.5°, which can reciprocate after every 24 min as a reference, $\theta = 15°$, 30°, 45°, 60°, 70°, and 75.5°). The feed speed was set to $f_p = 10$ mm/min ($f_p = (f_y{}^2 + f_z{}^2)^{1/2}$) in the θ-direction to be the same at all angles θ.

The theoretical polishing amount M [mg] for each angle θ under this experimental condition was obtained by using the Preston equation, as shown in Eq. (2). Considering the workpiece shape shown in **Fig. 14**, the paste collided with the workpiece side again before spreading in the radial direction, because it was separated from the workpiece side and was influenced more by the rotational frequency than by the centrifugal force. The paste was thought to rotate with the shape of region II (a circle of radius $R = 2.3$ mm), and the polishing radius in **Fig. 6(a)** is $R = 2.3$ mm. The graph in **Fig. 25** was obtained by calculating the theoretical polishing amount of the step by using the same procedure as that used for obtaining the theoretical polishing amount of a plane with the integration range of dx in Eq. (2) being $0 \leq x \leq 2.3$ mm. As the Preston coefficient must be determined experimentally, the experimental value obtained at the time of planar polishing was used. The polishing force was measured using a dynamometer. In addition, the paste at the time of polishing was observed through the acrylic plate from the back side, and the contact area was calculated. The relative polishing rate was assumed to be the speed of the rotation of the tool around the contact part. Preston constants were determined experimentally by measuring the mass change in the workpiece before and after processing. **Fig. 25** shows that the polishing amount increased with a decrease in angle θ. However, as shown in **Fig. 24**, the periodic interval of the vertical movement decreased with an increase in angle θ of the path. In other words, the interval between ascending and descending decreased and the polishing ranges overlapped such that the same place was polished multiple times. **Fig. 26** also shows that pressing force (load) F_z [N] for each gap G_t [mm] decreased rapidly at $G_t \geq 0.6$ mm and approached almost zero. As the pressing force significantly affected the polishing amount, the polishing amount for each gap also tended to be small. Regardless of the angle, the polishing time was short for large pressing force F_z (= large amount of grinding, $G_t = 0.3$–0.5 mm), and for a small F_t (= small amount of grinding, $G_t = 0.6$–1.3 mm). The same degree of the polishing effect was obtained under every condition. However, when angle θ was large, a sufficient polishing effect could be obtained by the overlapping of polishing because the overlapping ratio of the paths was large. In contrast, when angle θ was small, the overlapping ratio of the routes was also small; hence, the polishing effect was considered to be small. The graph showing the amount of theoretical polishing also considered that the polishing amount increased with an increase in the angle. Therefore, the theoretical polishing amount for the sinusoidal polishing path was obtained by considering the overlapping of polishing paths.

The overlap of the vertical and polishing paths greatly affected the polishing amount. Accordingly, Eq. (2) can be rewritten as

$$M_\theta = \frac{h}{10Y_b} \cdot \frac{C_e}{C_t} \cdot 4ky \int_0^R \int_0^T Pv \, dtdx, \quad \ldots \quad (10)$$

where Y_b [mm] is the distance traveled in the feed direction (Y-axis direction) per half cycle, C_e [mm^2] is the overlapping area of the half cycle, and C_t [mm^2] is the polishing area of the half cycle. The value achieved by obtaining theoretical polishing amount M_θ [mg] for each angle θ by using Eq. (10) is shown by the solid line in **Fig. 27**.

4.5.2. Experimental Results of Oscillation-Based Magnetic Polishing

Figure 28 shows the experimental result of the step surface, as well as the polishing amount, with 1-mm height

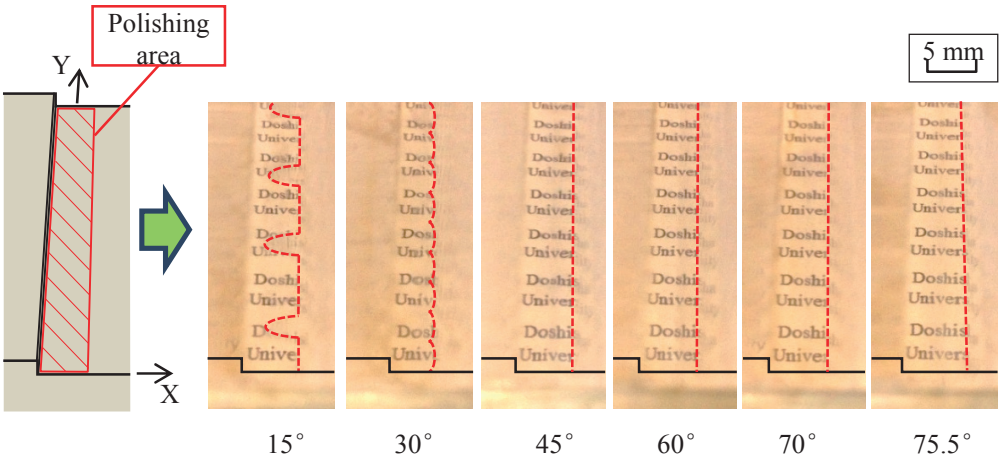

Fig. 28. Surfaces after polishing.

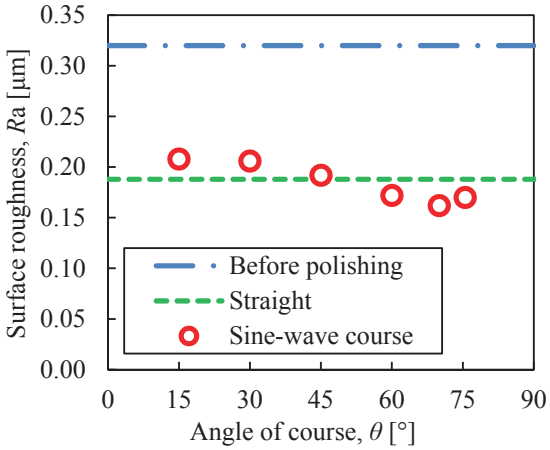

Fig. 29. Surface roughness versus course angle.

after polishing. The polished and unpolished portions can both be observed in the figure. The polishing tool diameter was $R_p = 2$ mm, and the gap between the workpiece side and the tool was $G_s = 0.3$ mm, with a polishing width of 4.6 mm. The right side of the dotted line in **Fig. 28** shows the unpolished part, which is outside the polishing range. However, the part within the polishing range was not polished even at $\theta = 15°$ and 30° because the angles were small. The portion where the polishing pressure decreased was considered to be the unpolished portion because the interval of the unpolished portion was coincidental with the period of the sinusoidal wave. The boundary between the polished and unpolished portions is clearly separated with an increase in angle θ. The polishing amount in **Fig. 27** depicts that the larger the angle θ, the higher is the polishing effect. **Fig. 27** also shows that the path duplication was considered effective in predicting the amount of polishing by the sinusoidal path because the trend of the experimental value coincided with that of the theoretical value. **Fig. 29** depicts the measurement result of the surface roughness *Ra*. Again, as the side polishing was not achieved, the roughness of the mirror-finished part of the bottom surface was measured. The results showed that the surface roughness along the "sinusoidal-wave path" was more improved than that along a "straight line" at approximately $\theta \geq 60°$; therefore, this value was effective in improving the polishing effect. In addition, $\theta = 60°$ was the angle of an appropriate triangle wave approximation because a longer polishing distance could be considered. In side grinding by using a ball-end mill-type grinding stone with a small diameter, the finished surface roughness was generally improved by the addition of an appropriate oscillation motion to the feed motion. Magnetic polishing seemed to have been affected by the elimination of the paste pool at the corner portion of the groove. It was also effective in improving the roughness of the finished surface of the bottom or corner portions.

5. Conclusion

In this study, the magnetic-polishing method was applied by using a ball-end mill-type tool with a small diameter to investigate the mirror-finish processing method for the microchannel groove-step and stepped shapes of a milling machine with a corner feature. The following conclusions were obtained from this study.

(1) The magnetic-polishing paste accumulated in the corner portion with respect to the uneven shape; hence, a sufficient polishing effect could not be obtained under the same polishing passage and condition as those of the flat surface. For the groove shape, the interior of the groove was not polished irrespective of the number of revolutions. In contrast, for the step shape, the polishing effect was slightly improved when the revolution number was reduced.

(2) The results, including magnetic polishing of the step shape made of acrylic and the observation of the magnetic-paste motion, showed that for an excessive amount of paste with respect to the work shape, the paste accumulates in the corner portion of the step,

and the following paste inhibits rotation. Furthermore, the paste rotation beneath the tool stopped intermittently because of the inhibiting paste.

(3) When the relationship between the step height h and diameter R_p of the polishing tool was represented as $\varepsilon = h/R_p$, the paste accumulation was observed for approximately $\varepsilon \geq 0.45$. This accumulation can be eliminated by the magnetic force of the tool by vertically applying an appropriate vertical motion at regular tool feed intervals.

(4) In the magnetic polishing of a shape, including the corner portion of the step, paste accumulation was not generated with the application of an appropriate oscillation motion perpendicular to the tool feed. The finished surface roughness of the bottom and corner portions could also be improved.

References:

[1] S. Okoma, "A history of computer development," Kyoritsu Shuppan, 2005 (in Japanese).
[2] M. Sakagami, "Latest Trends in Foreign Injection Molding Machines and Technologies (Part 1) Accelerating Eco-Molding," Pursuing Efficiency, and Improving Productivity Through Process Integration, Plastics age, Vol.61, No.10, pp. 90-95, 2015 (in Japanese).
[3] R. Neugebauer, M. Wabner, H. Rentzsch, and S. Ihlenfeldt, "Structure principles of energy efficient machine tools," CIRP J. of Manufacturing Science and Technology, Vol.4, Issue 2, pp. 136-147, 2011.
[4] Y. Okazaki, T. Mori, and N. Morita, "Desk-top NC milling machinewith 200 krpm spindle," Proc. 2001 ASPE Annual Meeting, pp. 192-195, 2001.
[5] M. Honiden, "A study of production optimization by cell production system for assembly," Japan Society for Production Management, Vol.10, No.2, pp. 181-186, 2004 (in Japanese).
[6] T. Hirogaki, E. Aoyama, K. Ogawa, T. Niiyama, M. Suzuki, and M. Iwama, "Estimation of environmental impact on desktop size five-axis control machine tools by LCA," Trans. of the Japan Society of Mechanical Engineers, Series C, Vol.75, No.52, pp. 371-378, 2009 (in Japanese).
[7] T. Hirogaki, E. Aoyama, K. Ogawa, and T. Niiyama, "Environmental Impact of Desktop-Sized Five-Axis CNC Machine Tool Estimated with LCA," Trans. of the JSME, J. of Environment and Engineering, Vol.6, No.2, pp. 242-252, 2011.
[8] L. Ma, T. Furuki, T. Kure, T. Hirogaki, and E. Aoyama, "Development of Polishing Tool Capable of Self-Adaptive to Processing Site using Steel Balls and Magnetic Force," Advanced Materials Research, Vol.806, pp. 466-471, 2015.
[9] L. Ma, T. Furuki, W. Wu, T. Hirogaki, and E. Aoyama, "Elucidation of the polishing mechanism by the magnetic polishing brush," Trans. of the JSME, 2016 (in Japanese).
[10] W. Wu, L. Ma, W. Wu, T. Hirogaki, E. Aoyama, M. Ikegaya, T. Echizenya, and S. Hirayoshi, "Study on Oil Adsorption and Polishing Characteristics by Novel Nanofiber Pad for Ultra-Precision Abrasive Machining," Int. Manufacturing Science and Engineering Conf., 2017, V001T02A043, 2017.
[11] H. Murakami, T. Furuki, E. Aoyama, T. Hirogaki, and K. Ogawa, "A33 Consideration about the Magnetic Polishing by End Mill shaped Tool at the Bottom of Micro Channel," The Japan Society of Mechanical Engineers, Vol.10, pp. 49-50, 2014 (in Japanese).
[12] M. Anzai, T. Nakagawa, N. Yoshioka, and S. Banno, "Development of Inline Micro-Deburring Applying Magnetic-Field-Assisted Polishing," Int. J. Automation Technol., Vol.4, No.1, pp. 9-14, 2010.
[13] K. Takahashi, "Deburring Finishing Using a Magnetic Polishing Machine," Int. J. Automation Technol., Vol.4, No.1, pp. 33-37, 2010.
[14] E. Aoyama, T. Hirogaki, K. Ookubo, K. Ogawa, K. Sawa, S. Ogawa, and R. Kawai, "Surface generation for Makyoh magic-mirror by end-milling with digitally functioned CNC machining center and magnetic polishing," J. of the Japan society for Abrasive Technology, Vol.55, No.9, pp. 540-545, 2011 (in Japanese).
[15] Y. Takebayashi, T. Hirogaki, E. Aoyama, K. Ogawa, and S. Melkote, "Application of Magnetic Polishing With Ball Nose Shaped Tool for Microchannel Shape," ASME J. of Micro and Nano-Manufacturing, Vol.2, No.2, 021009-1-9, 2014.
[16] F. W. Preston, "The Theory and Design of Plate Glass Polishing Machine," J. of Glass Technology, Vol.11, No.44, pp. 214-256, 1927.
[17] N. Yasunaga, "Polishing for the first time," Tokyo Denki University, pp. 84-85, 2011 (in Japanese).
[18] T. Nakajo, K. Nakano, and Y. Sawachika, "Measurement for micro shape by reflected light displacement," Report of the Tokyo Metropolitan Industrial Technic Institute, Vol.27, 4434477, 1995 (in Japanese).
[19] M. Hirono and K. Tsunoda, "Turning surface glossiness of aluminum alloys," The Japan Institute of Light Metals, Vol.35, No.10, pp. 581-587, 1985 (in Japanese).
[20] H. Nakagawa, T. Hirogaki, Y. Iwasaki, T. Hayashi, Y. Kita, and Y. Kakino, "Study on oscillation grinding by numerical control with a machining center," J. of the Japan Society for Precision Engineering, Vol.68, No.7, pp. 923-927, 2011 (in Japanese).

Name:
Yuki Manabe

Affiliation:
Doctor Course Student, Doshisha University

Address:
1-3 Tataramiyakodani, Kyotanabe-shi, Kyoto 610-0394, Japan
Brief Biographical History:
2016- Master Course Student, Doshisha University
2018- Doctor Course Student, Doshisha University

Name:
Hiroki Murakami

Affiliation:
Department of Mechanical and Systems Engineering, Doshisha University

Address:
1-3 Tataramiyakodani, Kyotanabe-shi, Kyoto 610-0394, Japan
Brief Biographical History:
2016- Morigo Seiki Co., Ltd.

Name:
Toshiki Hirogaki

Affiliation:
Professor, Faculty of Science and Engineering, Doshisha University

Address:
1-3 Tataramiyakodani, Kyotanabe-shi, Kyoto 610-0394, Japan

Brief Biographical History:
1990- Mitsubishi Motors Corporation
1993- Technology Research Institute of Osaka Prefecture
1995- The University of Shiga Prefecture
2006-2007 Visiting Researcher, University of California, Berkeley
2003- Doshisha University

Main Works:
• "Environmental Impact of Desktop-Sized Five-Axis CNC Machine Tool Estimated with LCA," J. of Environment and Engineering, Vol.6, No.2, pp. 242-252, 2011.
• "Control of Percussion Motion by Sound Feedback with a Humanoid Robot," Int. J. of Key Engineering Materials (Emerging Technology in Precision Engineering XIV), Vols.523-524, pp. 699-704, 2012.
• "Investigation of Temperature Hysteresis on Tooth Contact Surface of Hypoid Gears using Middle-infrared ray Imagery Based on Thermal Network model," J. of Advanced Mechanical Design Systems and Manufacturing, Vol.8, No.3, Paper No.13-00319, pp. 1-15, 2014.
• "Investigation of Step Micro-drilling Motion Based on Modeling of High Speed Spindle Driving Axis on Machine Tools Equipped with Vibration-Proof Mechanism," J. of Advanced Materials Research, Vol.1017, pp. 642-647, 2014.

Membership in Academic Societies:
• Japan Society of Mechanical Engineering (JSME)
• Japan Society for Precision Engineering (JSPE)
• Japan Society of Materials Science (JSMS)
• Japan Institute of Electronic Packaging (JIEP)

Name:
Eiichi Aoyama

Affiliation:
Professor, Faculty of Science and Engineering, Doshisha University

Address:
1-3 Tataramiyakodani, Kyotanabe-shi, Kyoto 610-0394, Japan

Brief Biographical History:
1977- Technology Research Institute of Osaka Prefecture
1997-1998 Visiting Researcher, Queen Mary & Westfield College, University of London
1987- Doshisha University

Main Works:
• "Estimation of Micro-hole Shape in Laser Direct Drilling of High Heat Radiation Typed Printed Circuit Boards (Process Monitoring with a High Speed Camera)," J. of Key Engineering Materials (Precision Engineering and Nanotechnology V), Vol.625, pp. 172-177, 2014.
• "An Indicative End-milling Condition Decision Support System Using Data-Mining for Difficult-to-cut Materials Based on Comparison with Irregular Pitch and Lead End-mill and General Purpose End-mill," J. of Advanced Materials Research, Vol.797, pp. 177-182, 2013.
• "Surface Generation for Magic-Mirror by End-Milling and Magnetic Polishing with Digitally Functioned CNC Machining Center," J. of Key Engineering Materials (Emerging Technology in Precision Engineering XIV), Vols.523-524, pp. 368-373, 2012.

Membership in Academic Societies:
• Japan Society of Mechanical Engineering (JSME)
• Japan Society for Precision Engineering (JSPE)
• Japan Society of Abrasive Technology (JSAT)
• Japan Society of Materials Science (JSMS)

Name:
Tatsuya Furuki

Affiliation:
Assistant Professor, Department of Mechanical Engineering, Gifu University

Address:
1-1 Yanagido, Gifu 501-1193, Japan

Brief Biographical History:
2016- Assistant Professor, Gifu University

Main Works:
• "Investigation of cBN electroplated end-mill shape for CFRP machining," Materials Science Forum, Vol.874, 2016.
• "End-milling of CFRP/Ti-6Al-4V with Electroplated cBN tool," Advanced Materials Research, 2015.

Membership in Academic Societies:
• Japan Society of Mechanical Engineers (JSME)
• Japan Society for Precision Engineering (JSPE)
• Japan Society of Abrasive Technology (JSAT)